STEM CELLS®

REGENERATIVE MEDICINE

Differentiation of Vascular Stem Cells Contributes to Ectopic Calcification of Atherosclerotic Plaque

ALEKSANDRA LESZCZYNSKA,[a,b] AIDEEN O'DOHERTY,[a] ERIC FARRELL,[a,c] JANA PINDJAKOVA,[a,d] FERGAL J. O'BRIEN,[e,f,g] TIMOTHY O'BRIEN,[a] FRANK BARRY,[a] MARY MURPHY[a]

Key Words. Mesenchymal stem cells • Vascular progenitor cells • Pericytes • Atherosclerosis • Vascular calcification • Chondrogenesis • Endochondral ossification • Collagen scaffold • In vivo

ABSTRACT

The cellular and molecular basis of vascular calcification (VC) in atherosclerosis is not fully understood. Here, we investigate role of resident/circulating progenitor cells in VC and contribution of inflammatory plaque environment to this process. Vessel-derived stem/progenitor cells (VSCs) and mesenchymal stem cells (MSCs) isolated from atherosclerotic ApoE$^{-/-}$ mice showed significantly more in vitro osteogenesis and chondrogenesis than cells generated from control C57BL/6 mice. To assess their ability to form bone in vivo, cells were primed chondrogenically or cultured in control medium on collagen glycosaminoglycan scaffolds in vitro prior to subcutaneous implantation in ApoE$^{-/-}$ and C57BL/6 mice using a crossover study design. Atherosclerotic ApoE$^{-/-}$ MSCs and VSCs formed bone when implanted in C57BL/6 mice. In ApoE$^{-/-}$ mice, these cells generated more mature bone than C57BL/6 cells. The atherosclerotic in vivo environment alone promoted bone formation by implanted C57BL/6 cells. Un-primed C57BL/6 VSCs were unable to form bone in either mouse strain. Treatment of ApoE$^{-/-}$ VSC chondrogenic cultures with interleukin (IL)-6 resulted in significantly increased glycosaminoglycan deposition and expression of characteristic chondrogenic genes at 21 days. In conclusion, resident vascular cells from atherosclerotic environment respond to the inflammatory milieu and undergo calcification. IL-6 may have a role in aberrant differentiation of VSCs contributing to vascular calcification in atherosclerosis. STEM CELLS *2016;34:913–923*

SIGNIFICANCE STATEMENT

Although chronic heart disease affects over 15 million patients in the United States alone, the pathophysiology of atherosclerosis and vascular calcification is not fully understood. Cues from this study hold promise to unfold the possible mechanisms underlying vascular calcification observed in atherosclerotic plaque. Our data indicates that the atherosclerotic environment has a fundamental effect on resident blood vessel stem/progenitor cells priming them to respond to the local inflammatory milieu to differentiate and calcify. Additionally, we have identified IL-6 as a potential inflammatory mediator. The role of IL-6 presented in this study provides implications for therapeutic applications to prevent vascular calcification.

INTRODUCTION

Vasculature has a notably high capacity for repair throughout embryonic and adult life with the presence of a number of stem progenitor niches and/or lineages described [1, 2]. That progenitor cells, producing cells of vessel walls in the embryo, remain within their niche and become activated to repair/regenerate the vascular wall in adults is a topic of active interest [3, 4]. Progenitor cell populations such as hemangioblasts, circulating endothelial progenitor cells, smooth muscle progenitor cells, mesenchymal stem cells (MSC) and pericytes in vessel walls have been isolated and characterized [4–7]. The demonstrated multipotency of these cells has led to their association with vascular calcification (VC) in atherosclerosis. VC is an important complication of atherosclerosis contributing to cardiovascular morbidity and mortality [8], given the increased risk of heart attack with calcified coronaries and the growing incidence of calcified aortic stenosis [9]. It is increasingly accepted that VC is far from a passive degenerative process but an active, organized, complex, and highly regulated process. In contrast to cardiac valvular and medial artery calcification, atherosclerotic-associated calcification is thought to occur by a process similar to endochondral ossification [10] with

[a]Regenerative Medicine Institute, National University of Ireland Galway, Galway, Ireland; [b]Division of Cardiology, Johns Hopkins University School of Medicine, Baltimore, Maryland, USA; [c]The Department of Oral and Maxillofacial Surgery, Special Dental Care and Orthodontics, Erasmus MC, University Medical Centre, Rotterdam, The Netherlands; [d]Integrated Center of Cellular Therapy and Regenerative Medicine, International Clinical Research Center, St. Anne's University Hospital, Brno, Czech Republic; [e]Tissue Engineering Research Group, Department of Anatomy, Royal College of Surgeons in Ireland, Dublin, Ireland; [f]Trinity Centre for Bioengineering, Trinity College Dublin, Dublin 2, Ireland; [g]Advanced Materials and Bioengineering Research (AMBER) Centre, RCSI & TCD, Dublin, Ireland

Correspondence: Mary Murphy, Ph.D., REMEDI, Biosciences Research, Dangan, National University of Ireland Galway, Galway, Ireland. Telephone: + 353 (0)91 495206; Fax: + 353 (0)91 495547; e-mail: mary.murphy@nuigalway.ie

Received June 8, 2015; accepted for publication October 30, 2015; first published online in STEM CELLS *EXPRESS* February 3, 2016.

1066-5099/2016/$30.00/0

http://dx.doi.org/10.1002/stem.2315

chondrocytes and osteoblasts detected in plaque [11]. In recent years, there has been growing interest in the role of resident progenitor cells as contributors to ectopic bone and cartilage formation. There is some evidence that resident vascular progenitor cells form nodules similar to calcified atherosclerotic plaques and get destabilized to factors like oxLDL akin to atherosclerotic plaques [12]. Moreover, similar to pericytes from other tissues, resident vascular pericytes have been shown to differentiate in aberrant tissues found in atherosclerotic plaque [13].

Here, we investigated the effect of the atherosclerotic environment on resident vessel-derived stem/progenitor cells (VSC) or bone marrow-derived MSC differentiation, representative of a circulating MSC population, in an attempt to elucidate their role in the formation of ectopic bone/cartilage in atherosclerotic plaque. The approach presented involved isolation and characterization of VSCs and MSCs from aortae and marrow, respectively, of normal, background C57BL/6 and atherosclerotic apolipoprotein E-null (ApoE$^{-/-}$) mice. Elements of plaque development such as early influx of inflammatory cytokines, formation of necrotic cores and accumulation of smooth muscle cells (SMCs) and fibrous tissue are similar to human disease in these mice [14]. The intrinsic capacity of the cell populations to form bone and the effect of the atherosclerotic host milieu on this process was assessed in vivo. Cells were loaded on a collagen-glycosaminoglycan scaffold [15] without priming or were first chondrogenically-primed in vitro. The effect of the atherosclerotic environment on bone formation was investigated by implanting both donor cell preparations into ApoE$^{-/-}$ recipient mice with constructs implanted in C57BL/6 mice as controls. The incidence, extent and quality of calcified cartilage and bone formation were assessed by a histological grading system.

In an attempt to understand the mechanism of ectopic vascular bone formation, the effect of pro-inflammatory cytokines found in atherosclerotic plaque was assessed at the molecular level. VSC preparations from C57BL/6 and ApoE$^{-/-}$ mice were induced to undergo chondrogenesis by exposure to transforming growth factor (TGF)-β3 and bone morphogenetic protein (BMP)-2 in a three-dimensional (3D) format in the presence or absence of interleukin (IL)-6, IL-1β or tumor necrosis factor (TNF)-α. The effect of the cytokines on temporal patterns of expression of characteristic matrix components during endochondral ossification was analyzed to identify the factors that potentially modulate vascular calcification in vivo.

Materials and Methods

MSC and VSC Isolation, Culture, and Characterization

All animal procedures were conducted in a fully accredited housing facility under a license granted by the Department of Health, Ireland and were approved by the Animal Care and Research Ethics Committee at the National University of Ireland Galway, Ireland. ApoE$^{-/-}$ MSCs were isolated as described previously with minor modifications [7]. Successful cultures of bone marrow-derived MSCs from C57BL/6 mice were established using modifications of a previously described procedure [16]. The isolation of VSC from ApoE$^{-/-}$ and C57BL/6 aortas was adopted from the protocol described by da Silva Meirelles and Nardi [7]. Briefly, dissected aortas with extraneous tissue removed were digested with collagenase twice with the second cell fraction used to establish cultures in RPMI-1640 medium with supplements. Subsequent to P2, cultures were transferred to MSC medium. Detailed information on isolation and growth analysis as well as isolation of fibroblasts is provided in Supporting Information.

Surface Marker Analysis

Cells at P6 were analyzed for surface marker expression using the FACSCanto (Becton Dickinson). Antibodies used for flow cytometry are listed in the Supporting Information. Data were analyzed by FlowJo software (Tree Star Inc.) using appropriate controls with isotype-matched IgG and unstained samples. Immunohistochemical staining for 3G5, a cell surface ganglioside typically found on vascular pericytes [17] was performed. 3G5 positive cells were purified from an ApoE$^{-/-}$ VSC preparation using fluorescence activated cell sorting as detailed in Supporting Information.

Multilineage Potential

MSCs and VSCs were evaluated for osteogenic, chondrogenic, and adipogenic differentiation. Osteogenic differentiation was assessed by determination of calcium phosphate deposition using von Kossa staining after 14 days in osteogenic differentiation medium [18] and calcium quantitation was assessed using Calcium Liquicolour Kit (StanBio, Boerne, TX). For adipogenic differentiation analysis, Oil Red O staining was performed on cells cultured for 20 days in adipogenic induction medium. For chondrogenesis, cell pellets were digested with papain and glycosaminoglycan (GAG) determined using the dimethylmethylene blue assay (DMMB). Histological sections (5 μm) of formalin-fixed pellets were stained for the presence of GAG using toluidine blue. Immunocytochemistry for type II and X Collagen was performed for establishment of the chondrogenic phenotype. All procedures are described in detail in the Supporting Information.

Animal Study and Histology

To study effects of the atherosclerotic environment and intrinsic capacity of the cells to differentiate in vivo, chondrogenically-primed constructs were implanted subcutaneously into C57BL/6 control and atherosclerotic ApoE$^{-/-}$ mice that had been fed a Western diet. The seeding of scaffolds and chondrogenic priming of constructs are detailed in Supporting Information methods.

For direct comparison, chondrogenically-primed, and control-unprimed constructs, loaded with either MSC or VSC from each mouse strain were implanted in C57BL/6 and ApoE$^{-/-}$ mice ($n = 8$ constructs). All mice were euthanized 8 weeks post-implantation and retrieved constructs were processed histologically. Four serial sections were cut at 4-8 levels at least 100 μm apart and stained with haematoxylin/eosin. To quantify bone formation in the implanted constructs, a robust histological grading/scoring system was developed to assess the extent of three distinct features of differentiation: calcified cartilage, bone, and bone marrow formation. Sections from each animal and each treatment were randomized to eliminate bias and scored for each feature by three independent, blinded researchers. The grading system involved assessment of bone formation by allotting an overall bone score on

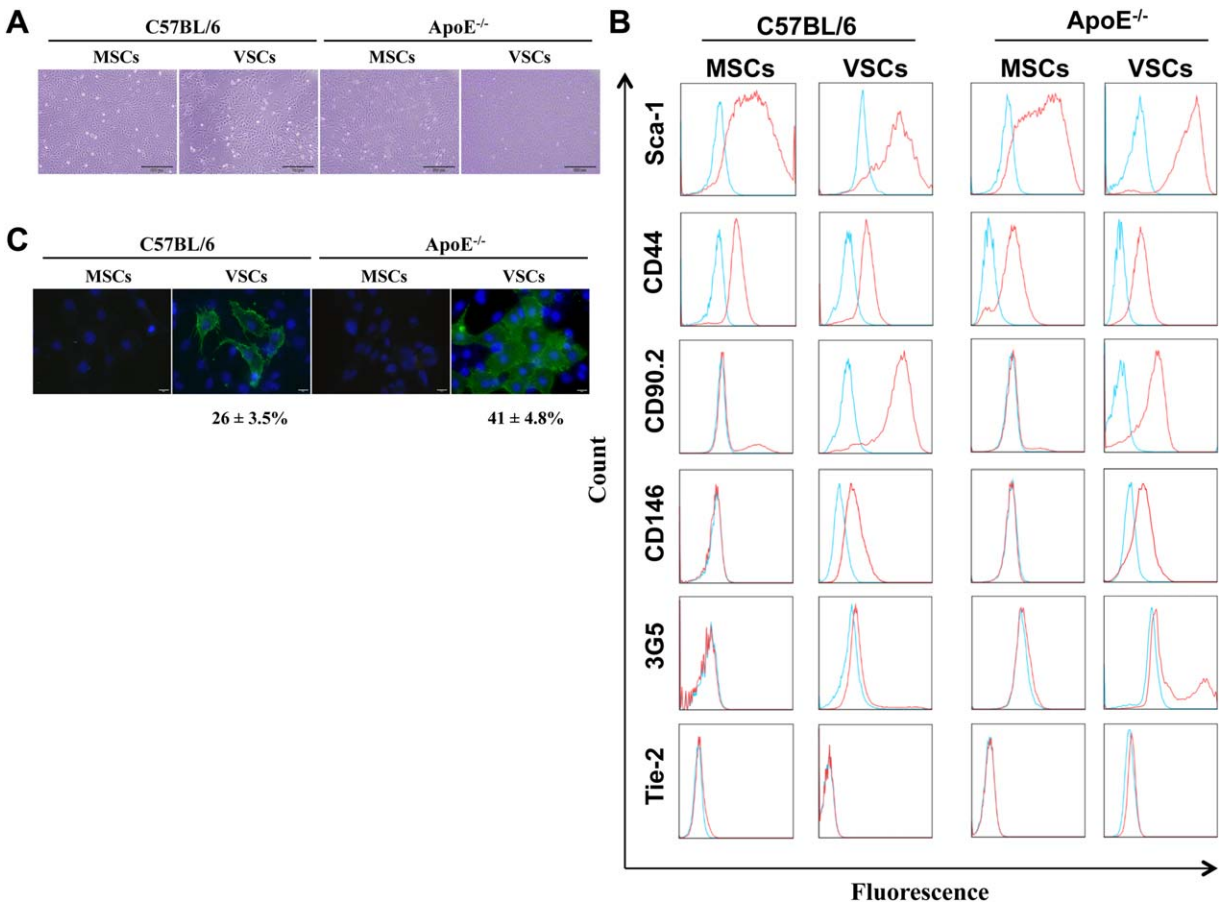

Figure 1. Characterization of isolated stem cell populations. **(A)**: Morphology of MSCs and VSCs isolated from ApoE$^{-/-}$ and C57BL/6 background mice. Representative images at P7 showed a characteristic spindle-like, fibroblastic appearance. Scale bar, 200 μm. **(B)**: Immunophenotypic profile of C57BL/6 and ApoE$^{-/-}$ MSCs and VSCs at P6. Surface marker expression (red line) for Sca-1, CD44, CD90.2, CD146, 3G5, and Tie-2 compared to respective isotype controls (blue line). **(C)**: Immunocytochemistry showing distribution of 3G5 positive MSCs and VSCs from both mouse strains; scale bar, 32 μm. Abbreviations: MSCs, mesenchymal stem cells; VSCs, Vessel-derived stem/progenitor cells.

the scale of 0–4 for the three parameters, with 0 indicating no tissue was detected and 4 indicating 100% fill of the construct. The overall bone score was defined as the sum of individual calcified cartilage, bone, and bone marrow scores. This bone score was used to define the percentage of overall bone formation with score of 4 set as 100%. The scoring system is detailed in Supporting Information Table 1. Sections were also stained with Safranin O and Collagen type X to visualize hypertrophic cartilage.

Effect of Pro-Inflammatory Cytokines on Chondrogenic Differentiation of VSCs

The effect of pro-inflammatory cytokines on chondrogenic differentiation of VSCs from ApoE$^{-/-}$ and C57BL/6 mice was assessed. Pellet cultures were established in chondrogenic medium with or without treatment with 200 ng/ml IL-6 [19], 1 ng/ml IL-1β [20] or 10 ng/ml TNF-α [20] (Peprotech) for 48 hours, and 7, 14, and 21 days. Gene expression of the chondrogenic markers Sox9, Fibromodulin, Type II collagen, Aggrecan (ACAN), Runx2, Alkaline phosphatase (ALP) and type X collagen was assessed. See Supporting Information data for detailed procedures.

Statistical Analysis

Data are expressed as the mean ± standard deviation (SD). All experiments were performed in triplicate, unless otherwise noted. Statistical significance was tested using Student's *t* test or ANOVA followed by Tukey's test. *p* value of $\leq .05$ was set as the cut off for statistical significance.

Results

Characterization of the Pericyte Nature of MSCs and VSCs

Bone marrow-derived MSCs and aorta-derived VSCs, isolated from C57BL6 and ApoE$^{-/-}$ mice showed a similar fibroblastic morphology (Fig. 1A). The proliferation profile of the cell populations was assessed from passage P6/7 to P14. Doubling times calculated for all three independent pooled preparations from ApoE$^{-/-}$ MSCs and VSCs as well as C57BL/6 VSCs show a strong similarity. C57BL/6 MSCs did display slower growth characteristics (Supporting Information Table 1). Assessment of mouse MSC-, pericyte-, hematopoietic-, and endothelial-associated cell surface markers was performed to define the surface signature of the isolated populations. Representative histograms for MSC and pericyte-associated

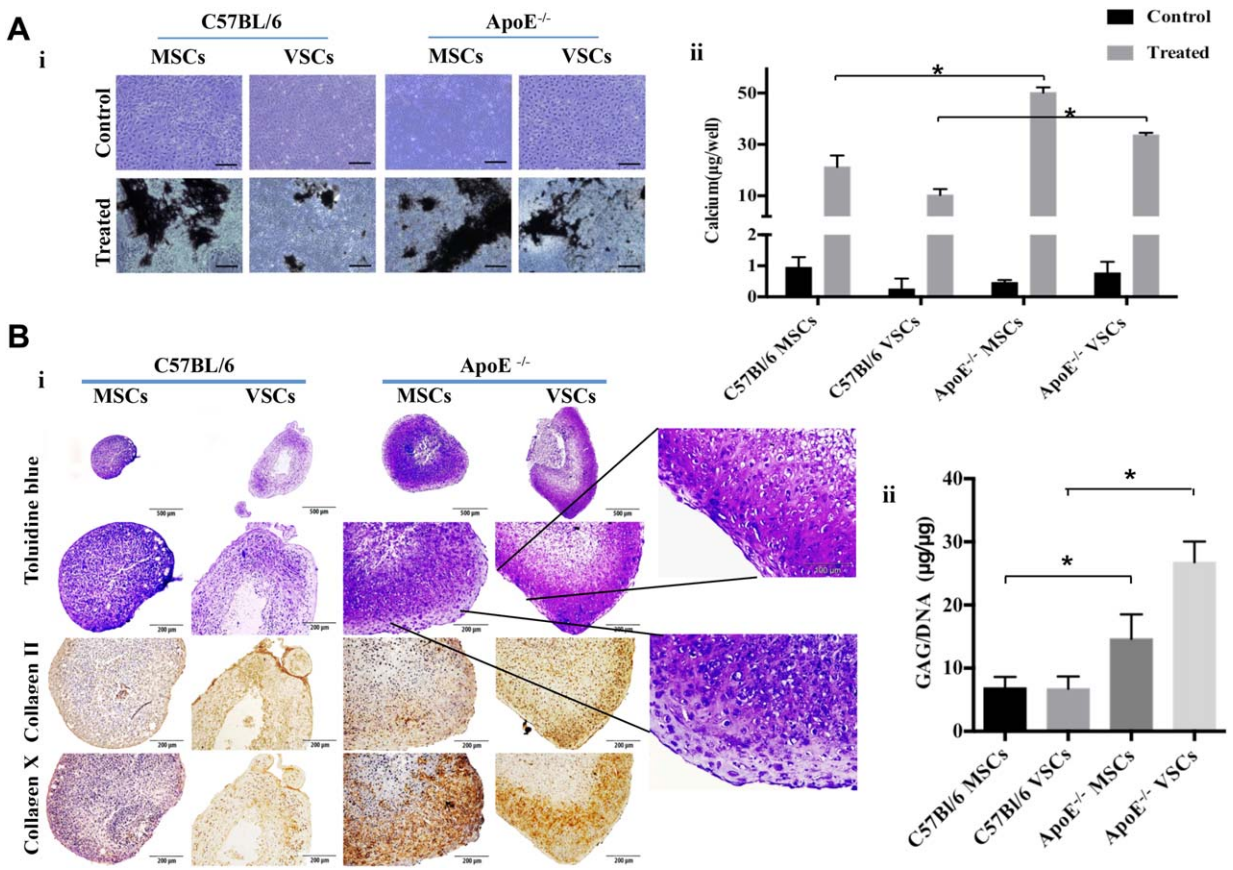

Figure 2. Osteogenic and Chondrogenic differentiation of stem cell populations. **(A)**: MSCs and VSCs isolated from C57BL/6 and ApoE$^{-/-}$ mice underwent osteogenesis as demonstrated macroscopically by positive Von Kossa staining (i) and quantitatively by assessment of calcium deposition (ii). Cells cultured in control medium were negative; scale bar, 500 μm. **(B):** (i) Chondrogenesis was assessed for proteoglycan deposition by toluidine blue staining after 21 days in pellet culture (top two panels with magnified insets taken from the regions indicated, scale bars 500 and 200 μm, respectively) and for the presence of collagen type II and X (scale bars, 200 μm). (ii) GAG/DNA ratios for isolated pellets ($n = 3$ cell preparations; *, **, $p \leq .05$). Abbreviations: MSCs, mesenchymal stem cells; GAG, glycosaminoglycan; VSCs, Vessel-derived stem/progenitor cells.

markers are shown in Figure 1B and Supporting Information Table 1 summarizes results obtained using three individual cell preparations. All VSCs and MSCs were negative for endothelial and hematopoietic cell markers but were positive for the previously described MSC markers Sca-1 [21, 22] and CD44 [21], although the latter was detected at a lower intensity (Fig. 1B). CD90.2 was detected in a low percentage of MSCs but present in VSCs. To further assess the pericyte nature of the cells, expression of the pericyte markers, CD146 and 3G5, was investigated (Fig. 1B, 1C). VSCs showed some positivity for CD146 while MSCs were negative. Likewise, the presence of 3G5 was associated with VSCs, although detected at lower levels by both flow cytometry (Fig. 1B) and immunofluorescent staining of cultured cells (Fig. 1C). Conversely, CD140b was detected at high levels in both MSC preparations (>90%) but at lower levels in C57BL/6 VSCs (57.2%) compared to Apo$^{-/-}$ VSCs (70.2%) (Supporting Information Table 2 and Figure 1). All MSC and VSC preparations were negative for Tie-2 (Fig. 1B).

The In Vivo Atherosclerotic Environment Increases the Ability of VSCs and MSCs to Generate a Calcified Matrix In Vitro

The ability of MSCs and VSCs, isolated from ApoE$^{-/-}$ and C57BL/6 mice, to generate a calcified matrix through direct intramembranous ossification or endochondral ossification, via a cartilage intermediate, was investigated. When treated with osteogenic supplements to induce direct ossification, all preparations showed the presence of a mineralized matrix by Von Kossa staining. Staining was more pronounced in VSCs and MSCs from ApoE$^{-/-}$ mice compared to cells from C57BL/6 mice (Fig. 2Ai and Supporting Information Figure 2). Quantification of calcium elaborated in the matrix indicated that levels were significantly higher in cells from ApoE$^{-/-}$ mice compared to the respective cells from C57BL/6 mice (Fig. 2Aii).

VSCs and MSCs from both mouse strains were induced to undergo chondrogenic differentiation by exposure to BMP-2 and TGF-β3 for 21 days in 3D culture, as a model for the first stages of endochondral ossification. In general, ApoE$^{-/-}$ MSC and VSC pellets tended to be larger in size compared to respective C57BL/6 pellets. The matrix generated was analyzed for GAG using toluidine blue staining and quantitation by DMMB. All treated preparations were positive for GAG with metachromatic staining in pellets generated from ApoE$^{-/-}$ cells comparatively more intense (Fig. 2Bi). At higher magnification, hypertrophic cells were observed to be embedded in the proteoglycan rich matrix.

Sequential sections from the center of pellets were immunostained for type II and type X collagen to confirm

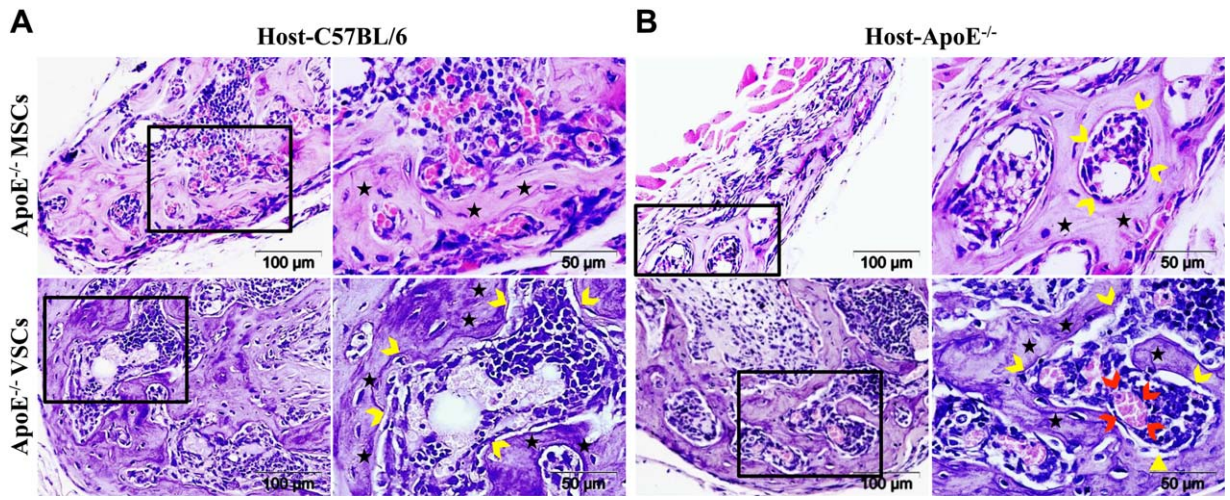

Figure 3. The atherosclerotic environment and bone forming capacity of isolated progenitors. **(A)**: All chondrogenically primed ApoE$^{-/-}$ MSC and VSC constructs retrieved from C57BL/6 mice showed mineralization and bone formation (black stars). **(B)**: Primed ApoE$^{-/-}$ MSC and VSC constructs retrieved from ApoE$^{-/-}$ mice showed more mature bone formation with well-developed bone marrow (yellow arrowheads) and blood vessels (red arrowheads) detected. Boxes indicated areas magnified. Left panels, 100 μm magnification; right panels, 50 μm). Abbreviations: MSCs, mesenchymal stem cells; VSCs, Vessel-derived stem/progenitor cells.

chondrogenesis and hypertrophic differentiation, respectively. Type II collagen staining was detected primarily in the periphery of MSC pellets but more generally expressed in VSC chondrogenic cultures. Localization of type X collagen correlated with type II collagen. Although all pellet cultures showed abundant accumulation of type II and X collagen at 21 days, staining appeared greater in the ApoE$^{-/-}$ MSC and VSC pellets (Fig. 2Bi). The GAG/DNA ratio in ApoE$^{-/-}$ MSC and VSC pellets was also significantly higher when compared to respective C57BL/6 pellets (Fig. 2Bii), indicating either increased synthesis and/or low turnover per cell. Overall, VSCs and MSCs from ApoE$^{-/-}$ mice had significantly higher in vitro chondrogenic potential compared to control mice. Fibroblasts, isolated from adult ApoE$^{-/-}$ and C57BL/6 mouse skin and lung tissue, did not undergo osteogenesis and formed loose pellets that were not possible to evaluate for chondrogenic differentiation.

Supporting Information Figure 3 shows negative staining for calcium post osteogenic differentiation of ApoE$^{-/-}$ and C57BL/6 lung fibroblasts. ApoE$^{-/-}$ MSCs, used as a positive control, were positive for both osteo- and chondrogenesis (results not shown).

As 3G5 positive cells (3G5^{+}) have been shown to differentiate to bone and cartilage [23], 3G5^{+} and 3G5^{-} VSCs were sorted to 100% purity and compared to the parent ApoE$^{-/-}$ VSC population with respect to chondrogenic differentiation. The parent and sorted cell populations were expanded for two passages to obtain sufficient cell numbers and exposed to chondrogenic medium for 21 days. 3G5^{+} cells formed a cohesive pellet with positive metachromatic staining and hypertrophic cells detected (white arrow). Parent cells also showed positive GAG staining. Conversely, 3G5^{-} cells formed a loose pellet compared to the 3G5^{+} pellets with weak GAG staining. With respect to GAG/DNA levels, 3G5^{+} cells produced over 1.5 fold more GAG than the parent and 3G5^{-} cells (12.3 ± 0.4, 8.1 ± 0.1, and 7.2 ± 0.5 $\mu g/\mu g$ GAG/DNA, respectively) (Supporting Information Figure 4).

Following adipogenic differentiation, accumulation of lipid droplets was visualized in C57BL/6 MSCs using Oil Red O staining whereas ApoE$^{-/-}$ MSCs and VSCs were negative for adipogenic differentiation (data not shown).

Assessment of the Intrinsic Calcification Capacity of Progenitor Cells In Vivo and the Effect of the Atherosclerotic Environment

To assess calcification of progenitor cells in vivo, passage (P)8 MSCs and VSCs from both mouse strains were loaded on collagen-glycosaminoglycan scaffolds [15] and predifferentiated in chondrogenic medium for 32 days prior to subcutaneous implantation. Cell-scaffold constructs maintained in control culture medium for 32 days served as negative controls. A crossover experimental plan was used where cells from each strain were implanted in C57BL/6 and ApoE$^{-/-}$ mice (Supporting Information Figure 5).

Control and chondrogenically-primed constructs were stained with toluidine blue to assess the quality of seeding. Cells were found distributed throughout the constructs; however, cell density was higher at the edges. In all seeded, chondrogenically-primed constructs, weak matrix staining for GAG was evident whereas the controls showed no GAG deposition (Supporting Information Figure 6). Not all implanted constructs were retrievable with control cultures recovered at a lower frequency. The gross appearance of primed constructs is presented in Supporting Information Figure 7 with vascularization and a bony appearance evident. Representative sections were stained with Safranin O and collagen type X to confirm the appearance of hypertrophic cartilage (Supporting Information Figures 8 and 9).

ApoE$^{-/-}$ MSCs and VSCs Form Bone in C57BL/6 Mice

When chondrogenically-primed constructs from atherosclerotic mice were transplanted into subcutaneous pouches of control mice, all MSC- or VSC-seeded constructs underwent mineralization and formed bone (Table 1A and B, Fig. 3A). In the case of the primed ApoE$^{-/-}$ MSC constructs retrieved from C57BL/6 mice, 5 of 5 retrieved constructs had evident bone formation. The overall bone formation was 77.5% with

Table 1. Histological analysis of (A) MSC and (B) VSC constructs retrieved from ApoE$^{-/-}$ and C57BL/6 mice scored for bone, calcified cartilage and bone marrow formation

A

Host			Implanted cells: ApoE $^{-/-}$ MSCs control	ApoE $^{-/-}$ MSCs primed	C57BL/6 MSCs control	C57BL/6 MSCs primed
ApoE $^{-/-}$		Calcified Cartilage	2/4 (0.41)	5/5 (0.94)	1/5 (0.12)	3/5 (0.37)
		Bone	2/4 (0.12)	5/5 (1.2)	2/5 (0.08)	2/5 (0.24)
		Bone Marrow	2/4 (0.19)	5/5 (0.6)	0/5 (0)	1/5 (0.14)
		Overall Bone Score	0.72	2.74	0.2	0.75
		Percentage of overall bone formation	18%	68.5%	5%	18.75%
C57BL6		Calcified Cartilage	0/4 (0)	5/5 (1.27)	0/4 (0)	1/4 (0.23)
		Bone	0/4 (0)	5/5 (0.99)	0/4 (0)	1/4 (0.15)
		Bone Marrow	0/4 (0)	5/5 (0.84)	0/4 (0)	0/4 (0)
		Overall Bone Score	0	3.1	0	0.38
		Percentage of overall bone formation	0%	77.5%	0%	9.5%

B

Host			Implanted cells: ApoE $^{-/-}$ VSCs control	ApoE $^{-/-}$ VSCs primed	C57BL/6 VSCs control	C57BL/6 VSCs primed
ApoE $^{-/-}$		Calcified Cartilage	3/4 (0.32)	6/6 (0.96)	0/4 (0)	0/4 (0)
		Bone	3/4 (0.27)	6/6 (1.01)	0/4 (0)	0/4 (0)
		Bone Marrow	1/4 (0.13)	6/6 (1.36)	0/4 (0)	0/4 (0)
		Overall Bone Score	0.72	3.33	0	0
		Percentage of overall bone formation	18%	83.25%	0%	0%
C57BL/6		Calcified Cartilage	1/6 (0.023)	5/5 (1)	0/4 (0)	0/6 (0)
		Bone	0/6 (0)	5/5 (0.63)	0/4 (0)	0/6 (0)
		Bone Marrow	0/6 (0)	3/5 (0.71)	0/4 (0)	0/6 (0)
		Overall Bone Score	0.023	2.34	0	0
		Percentage of overall bone formation	0.583%	58.4%	0%	0%

Note: Constructs were stained with H&E staining for light microscopic evaluation and grading by three blinded reviewers. Numbers represent constructs showing the presence of the particular feature out of the total number of retrieved constructs. Numbers in brackets indicate the average score of the three assessments for the presence of bone, calcified cartilage and marrow and overall bone score the sum of these values. Overall bone formation was calculated from the summed mean scores with 4 representing 100% coverage.
Abbreviations: MSCs, mesenchymal stem cells; VSCs, Vessel-derived stem/progenitor cells

more than 20% of bone marrow formation suggesting areas of maturity. However, the presence of 25% calcified cartilage indicated areas of less mature bone. Chondrogenically-primed ApoE$^{-/-}$ VSC constructs retrieved from C57BL/6 mice formed bone or immature bone in 5 of 5 retrieved samples. In 3 of 5 constructs, bone marrow was seen (Fig. 3A). Of the 58.4% overall bone formation score, 25% was immature bone with calcified cartilage while 17.75% bone marrow was present. In summary, bone marrow-derived MSCs, with known bone forming capacity, demonstrated a greater capacity for bone formation post-chondrogenic priming than VSCs from the same atherosclerotic background.

The Atherosclerotic Environment Complements the Intrinsic Capacity of ApoE$^{-/-}$ MSCs and VSCs to Form Bone

To investigate how the intrinsic capacity of MSCs and VSCs from atherosclerotic mice is affected by the atherosclerotic environment, the fate of the ApoE$^{-/-}$ constructs in ApoE$^{-/-}$ mice was assessed. Quantification of overall bone formation is detailed in Table 1 (A and B). All five constructs of primed ApoE$^{-/-}$ MSCs retrieved from atherosclerotic mice formed bone and bone marrow. With prominent dense bone appearance (30%), calcified matrix (23.5%) and areas with bone marrow (15%), the overall bone formation was rated at 68.5%. A large number of hypertrophic cells were observed surrounded by cartilage-like matrix containing bone like tissue components and invading blood vessels (Fig. 3B and Table 1A). Of note, un-primed control ApoE$^{-/-}$ MSC constructs retrieved from atherosclerotic mice also formed some bone with 18% of overall bone formation and 10.25% cartilage observed in 2 of 4 retrieved constructs. Total bone marrow observed was 4.75% and seen in 2 of 4 retrieved constructs (Table 1A).

The examination of 6 of 6 primed ApoE$^{-/-}$ VSCs in the ApoE$^{-/-}$ environment showed the presence of osteoid tissue with a number of hypertrophic cells embedded in a cartilaginous matrix; notably, all constructs showed invading blood vessels (Fig. 3B and Table 1B). The bone appearance was dense with 83.25% overall bone formation and the presence of a calcified matrix was prominent with 24% coverage. In all treated ApoE$^{-/-}$ constructs retrieved from ApoE$^{-/-}$ mice, substantial formation of bone marrow was observed (34%), revealing the maturity of the developed bone. Similar to ApoE$^{-/-}$ MSCs explanted from atherosclerotic mice, unprimed ApoE$^{-/-}$ VSCs formed some bone (18%) in atherosclerotic mice (Table 1B). Detection of significant levels of calcified cartilage in both conditions suggested endochondral ossification as the primary pathway for bone formation. That both unprimed atherosclerotic MSCs and VSCs formed bone when exposed to the diseased environment and primed atherosclerotic VSCs generated about 25% more bone highlights the effect of the atherosclerotic environment on the calcifying potential of vessel progenitor cells.

The Atherosclerotic Environment Positively Impacts Bone Formation Capacity of C57BL/6 Cells

For ApoE$^{-/-}$ MSC (4 of 4) and C57BL/6 MSC (4 of 4) control constructs retrieved from control mice, there was no bone, cartilage, or bone marrow formation (Table 1A). Two of 5 C57BL/6 MSC control constructs retrieved from atherosclerotic mice had overall bone formation at 5%. Of this, 3% was calcified cartilage with no bone marrow observed (Fig. 4 and Table 1A). This analysis of nonatherosclerotic constructs retrieved from the atherosclerotic environment indicated a modest role of the atherosclerotic environment alone. In the case of primed C57BL/6 MSCs retrieved from atherosclerotic mice,

overall new bone formation was 18.75%. Two of five constructs formed some bone while 3 of 5 constructs showed an average of 9.25% calcified cartilage (Fig. 4 and Table 1A). However, un-primed C57BL/6 VSCs were unable to form bone in either mouse strain (Fig. 4, Table 1B) suggesting that vessel-resident progenitor cells do not have intrinsic capacity to form bone.

Effect of IL-6, IL-1β, or TNF-α on Pattern of Expression During Chondrogenesis

In vivo data highlighted the relevance of the source of progenitor cells to their calcification/bone formation potential, with the inflammatory milieu of the atherosclerotic ApoE$^{-/-}$ mouse altering the intrinsic calcification capacity of ApoE$^{-/-}$ cells. Short term implantation in this inflammatory environment also resulted in increased bone capacity of C57BL/6 MSCs, although not VSCs. To determine putative factors involved in establishing the atherosclerotic progenitor cell phenotype we investigated the effect of IL-6, IL-1β, and TNF-α on chondrogenesis of VSCs. Pellet cultures were established from ApoE$^{-/-}$ and C57Bl/6 VSCs and treated with chondrogenic induction medium supplemented with 200 ng/ml IL-6, 1 ng/ml IL-1β, or 10 ng/ml TNF-α treatment. Chondrogenically-cultured pellets without cytokine treatment acted as controls.

In terms of morphology, ApoE$^{-/-}$ and C57BL/6 VSC pellets treated with chondrogenic induction medium alone for 21 days and stained with toluidine blue had the characteristic blue-pink appearance indicating the presence of GAG (Fig. 5A). GAG/DNA levels were equivalent between the two populations (Fig. 5B, 5C). C57BL/6 VSC pellets treated with inflammatory cytokines were smaller in appearance with minimal GAG detected histologically and quantitatively (Fig. 5A, 5B). GAG/DNA levels were significantly reduced by exposure to IL-6, IL-1β, and TNF-α compared to controls. Treatment with 200 ng/ml IL-6 caused a reduction in GAG production; treatment with 1 ng/ml IL-1β or 10 ng/ml TNF-α further impacted chondrogenic differentiation of C57BL/6 VSCs with significantly reduced GAG levels compared to the IL-6-treated pellets (Fig. 5B).

After 21 days chondrogenic pellet culture in the presence of pro-inflammatory cytokines, ApoE$^{-/-}$ VSCs had a distinct chondrogenic appearance/morphology. Notably, the IL-6 treated pellets were larger than control cultures treated with chondrogenic medium alone (Fig. 5A). This increased size correlated with significantly higher GAG/DNA levels (Fig. 5C), whereas exposure to 1 ng/ml IL-1β or 10 ng/ml TNF-α had no effect compared to controls. Glycosaminoglycan deposition after exposure to IL-6 was significantly higher compared to all other treatments (Fig. 5C).

The effect of 200 ng/ml IL-6 on expression of the chondrogenic-associated molecules, Sox-9, and fibromodulin, as well as collagen type II and aggrecan at 21 days was found to be significantly higher in ApoE$^{-/-}$ VSCs compared to C57BL/6 VSCs treated with 200 ng/ml IL-6 (Fig. 6A-6D). Similarly, IL-6 addition led to a significant increase in gene expression of *Runx2* and *ALP*, markers of chondrocyte hypertrophy, in ApoE$^{-/-}$ VSCs compared to C57BL/6 VSCs at 21 days (Fig. 6E, 6F). Significance was also seen at day 2 for *Runx2* and day 7 for *ALP*. However, treatment with IL-6 led to decreased collagen type X expression, also associated with hypertrophy and generation of a transient cartilage template in endochondral ossification, in both ApoE$^{-/-}$ and C57BL6 VSCs compared to control cultures (Fig. 6G). The treatment with either IL-1β or TNF-α showed a trend toward decreased expression of all chondrogenic genes tested compared to control cultures (data not shown).

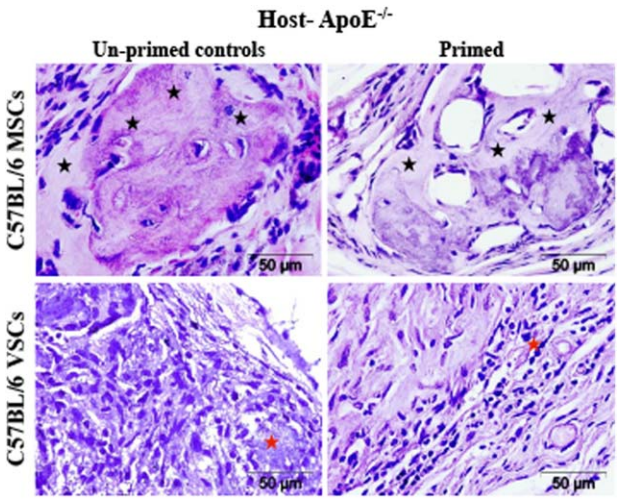

Figure 4. Effect of atherosclerotic environment on non-atherosclerotic C57BL/6 cells. Control, unprimed C57BL/6 MSC constructs implanted into ApoE$^{-/-}$ mice showed calcified cartilage and some bone formation (black stars). Comparatively, primed C57BL/6 MSC constructs showed more bone formation with marrow like spaces. Control and chondrogenically-primed C57BL/6 VSC constructs implanted in to ApoE$^{-/-}$ mice showed no bone formation while remnants of scaffolds (red stars) were seen. Scale bars, 50 μm. Abbreviations: MSCs, mesenchymal stem cells; VSCs, Vessel-derived stem/progenitor cells.

Discussion

In recent years, dogmas of not only repair and regeneration but disease progression are changing rapidly with identification of various stem/progenitor cells in the vessel wall. One target cell population is the MSC, described as a pericyte or pericyte-like cell and proposed to have a perivascular origin [6, 24, 25]. Although current knowledge of vessel-derived progenitor cells is in its infancy, much attention has focused on their therapeutic application for conditions such as myocardial infarction, ischemic heart disease, and limb ischemia. The contribution of altered stem or progenitor cell function to disease development is also of interest with reports of dysfunction in bone marrow-derived endothelial progenitor cells, fibrocytes, pericytes, MSCs, or smooth muscle progenitor cells contributing to atherosclerosis and vascular calcification [23, 26–29]. There is also increasing evidence that the vessel wall, including the vascular intima or adventitia, is the seat for resident stem progenitor cells [30] which can be induced to calcify [31]. Evidence also suggests the presence of progenitor cells in tunica media which can transdifferentiate into smooth muscle cells and contribute to vascular remodeling in atherosclerosis [32].

The aim of this study was to identify, isolate and characterize a population of resident stem/progenitor cells from the aortic wall of young atherosclerotic mice and to assess their role in the pathogenesis of atherosclerosis. VSCs were shown

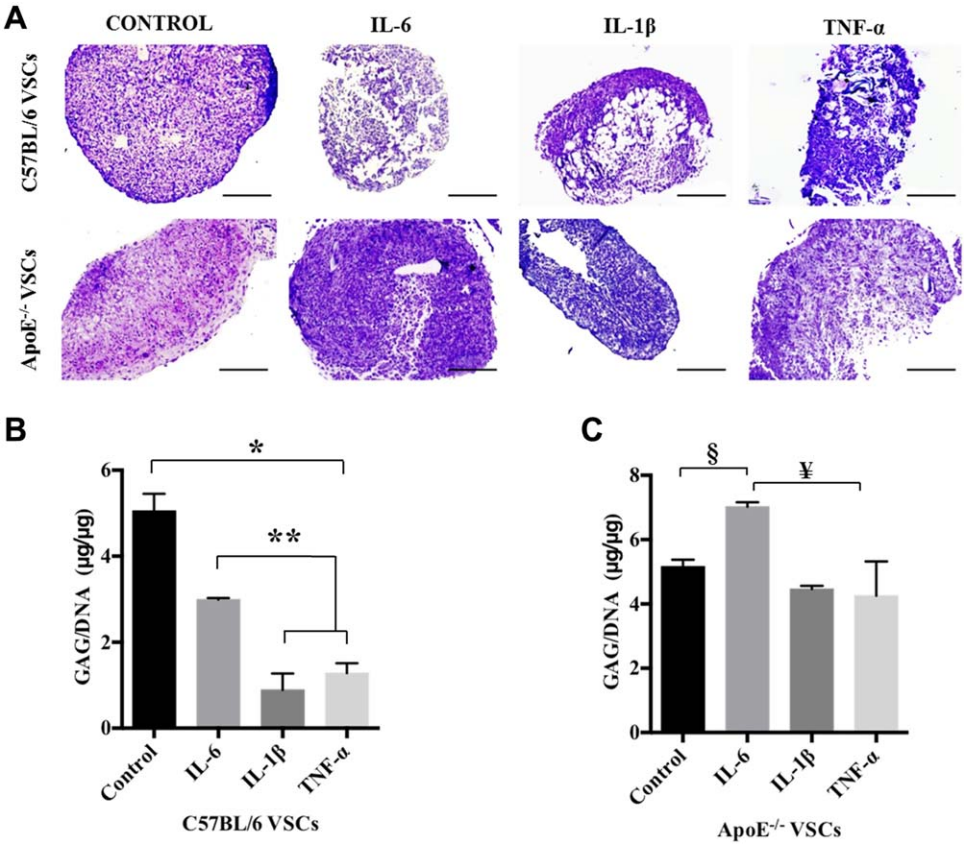

Figure 5. Effect of pro-inflammatory cytokines on chondrogenesis of ApoE$^{-/-}$ and C57BL/6 VSCs. **(A)**: The effect of treatment with IL-6 (200 ng/ml), for 21 days on proteoglycan deposition during chondrogenic differentiation of C57BL/6 and ApoE$^{-/-}$ VSCs is visualized by toluidine blue staining (Scale bars, 200 μm) and **(B)** quantified by determination of GAG/DNA ratio ($n = 3$ cell preparations; *, $p < .01$; **, $p < .02$; ¥, $p < .05$). Abbreviations: GAG, glycosaminoglycan; TNF-α, tumor necrosis factor; VSCs, Vessel-derived stem/progenitor cells.

to be capable of differentiating into bone and cartilage and were fundamentally altered by the atherosclerotic environment. These cells were compared to bone marrow-derived MSCs to elucidate their potential contribution to formation of ectopic bone or cartilage in atherosclerotic plaque. Resident progenitors were associated with a more pericyte-like phenotype compared to matched MSCs, circulating progenitor cells that may contribute to vascular calcification in plaque [33]. Indeed, both MSCs and VSCs from atherosclerotic mice were shown to display significantly higher capacity to form a cartilaginous template and directly ossify in vitro compared to control cells from non-atherosclerotic, wild type mice. However, ApoE$^{-/-}$ VSCs had a greater chondrogenic capacity than the same cells isolated from C57BL/6 mice. In vivo, formation of prominent and mature bone-like structures in chondrogenically-primed ApoE$^{-/-}$ VSC and MSC constructs, even in a non-atherosclerotic environment, suggested an intrinsic proclivity of these cells to form ectopic bone, which in the case of VSCs was boosted even further in the atherosclerotic environment. This notion was further supported by the observation that the MSCs from control mice, whether primed or not, were substantially less prone to form bone even in the atherosclerotic environment. In contrast to MSCs isolated from bone marrow which have a known functional role in bone formation, VSCs isolated from the aorta of C57BL/6 mice did not have the capacity to form bone or calcify in vivo indicating that these vessel-derived progenitors do not have bone forming capacity in the non-diseased environment. However, ApoE$^{-/-}$ VSCs that were primed to undergo chondrogenesis prior to subcutaneous implantation in control mice formed bone.

Metaplasia and calcification occurs in the aortic tunica. It is now known that this abnormality is not just a physical accumulation of calcium phosphate, but involves mechanisms similar to bone formation with a number of bone-related proteins expressed within the vessel wall [11]. The presence of calcified cartilage and bone in the majority of constructs where differentiation of implanted cells occurred, and particularly in unprimed constructs, suggests that endochondral ossification was the primary pathway involved. Differentiation and calcification of constructs in the atherosclerotic environment may be regulated by exposure to various factors like TNF-α or IL-6 which may also play role in formation of the plaque and atherogenesis [34]. To date, a number of researchers have reported the presence of stem cells in blood vessels including the aorta [7]. Their regenerative role in injury is well known, however, our work was based on the premise that they can also be implicated in pathological processes under certain conditions. The mechanism whereby this occurs is not fully understood. The potential of vessel wall stem cells to form bone, cartilage, muscle or fat has been reported previously [35]. More specifically, the cells which are isolated form aortic tunicae have a greater tendency to differentiate to the osteogenic lineage [35, 36] on exposure to inflammatory cytokines.

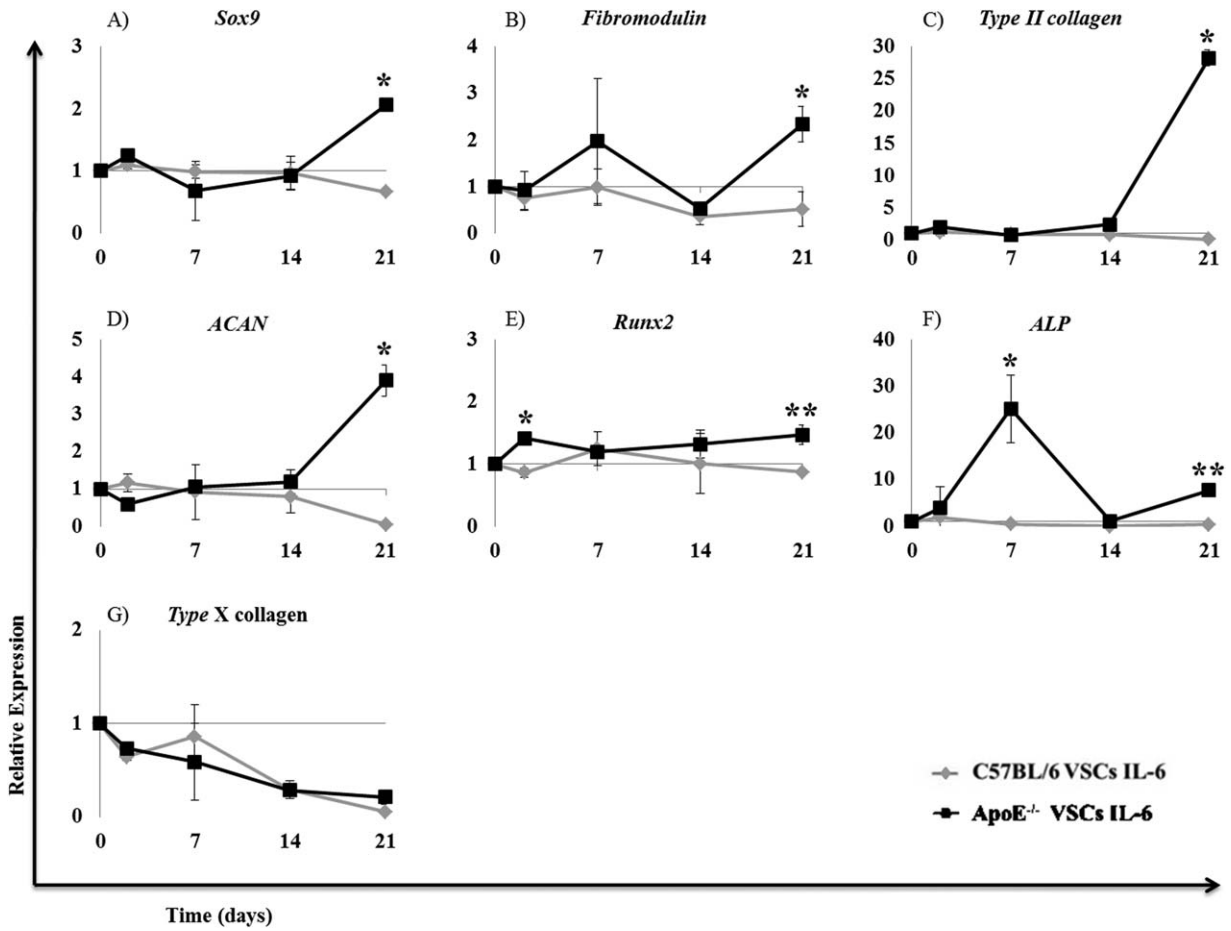

Figure 6. Effect of IL-6 on expression of representative chondrogenic genes during differentiation of ApoE$^{-/-}$ and C57BL/6 VSCs. Isolated cells were differentiated in chondrogenic conditions in the presence or absence of IL-6 (200 ng/ml) and cultured in pellet format for 21 days. Gene expression normalized to GAPDH of **(A)** Sox9, **(B)** fibromodulin, **(C)** type II collagen, **(D)** ACAN, **(E)** Runx2, **(F)** ALP, and **(G)** type X collagen at time 0, and 48 hour, 7 day, 14 day, and 21 day pellets ($n = 5$) in chondrogenic medium. Data represents the relative expression seen after exposure to IL-6 compared to control cultures exposed to chondrogenic medium without IL-6 ($n = 3$ cell preparations, two technical replicates; *, $p < .03$; **, $p < .02$). Abbreviations: ACAN, Aggrecan; ALP, Alkaline phosphatase; VSCs, Vessel-derived stem/progenitor cells.

In both environments, ApoE$^{-/-}$ cells were prone to calcify and develop bone structures; nevertheless VSCs were more sensitive to environmental factors. The ApoE$^{-/-}$ environment seemed to contribute to mature bone formation in the ApoE$^{-/-}$ primed constructs but to a lesser degree in control nonprimed constructs. Interestingly, the ApoE$^{-/-}$ environment also triggered bone formation in C57BL/6 control constructs, even without priming, albeit to a much lesser degree, again supporting the hypothesis that the atherosclerotic environment plays a role in differentiation and ectopic bone formation. The importance of the atherosclerotic environment in bone formation becomes even more obvious by the observation that control constructs retrieved from the control non-atherosclerotic environment did not form bone. Nevertheless, the finding that there was some bone formation in primed C57BL/6 constructs retrieved from control mice, was similar to findings in Balb/C mice [37] and rats [38]. Previously, it has been shown that cells subjected to differentiation assays will usually downregulate bone and chondrogenic transcription factors under pro-inflammatory conditions [20]. In this study, we found that the pro-inflammatory environment of the atherosclerotic mice did not inhibit the formation of bone in subcutaneous implants but exaggerated the effect leading to more advanced calcification, particularly in the case of VSCs. In the atherosclerotic environment, a number pro-inflammatory cytokines such as TNF-α, IL-6, IL-1β are increased [39] and inflammatory cytokines are strongly related to ectopic bone formation [40].

What triggers the inflammatory reaction in atherosclerosis is not completely understood. However, numerous factors such as oxidized LDL, free oxygen radicals and to some extent, MMPs, heat shock proteins, and advanced glycation end products have been implicated. Data presented here help to understand the regulatory mechanisms that link pericytes/VSCs and ectopic calcification. Although the role of factors other than inflammatory cytokines in promoting bone formation or calcification in vivo cannot be ignored, the significant inhibitory effect of IL-6, IL-1β and TNFα on proteoglycan production in C57BL/6 control VSC chondrogenesis in vitro compared to no effect of IL-1β and TNFα and significantly increased chondrogenic and hypertrophic gene expression as well as overall GAG levels in response to IL-6 in ApoE$^{-/-}$ VSCs does indicate that these pro-inflammatory cytokines, upregulated in the atherosclerotic environment, can modulate VSC chondrogenesis. Overall, there was over twofold more GAG/DNA produced by ApoE$^{-/-}$ VSCs compared to control

C57BL6 VSCs. Similarly, Lacey et al. have demonstrated that mouse MSCs, differentiated in the presence of pro-inflammatory cytokines, had decreased chondrogenic and osteogenic gene expression and both IL-1β and TNF-α have been shown to significantly inhibit chondrogenesis of human MSCs [20, 41, 42]. Furthermore, these factors potently inhibit expression of Sox 9, the master chondrogenic transcription factor through the NF-κB pathway [43]. As for control C57BL/6 VSCs, IL-6 has also been shown to inhibit chondrogenesis of healthy human MSCs [44, 45]. In this study, we have shown for the first time that the Lacey VSCs have the ability to respond to IL-6 treatment and induce accumulation of proteoglycans. The difference between Lacey VSCs and C57BL/6 VSCs was also apparent visually with IL-6-treated Lacey VSC pellets appearing larger than control cultures in contrast to the TNF-α and IL-1β treated pellets. IL-6 has also been shown to induce calcification of SMCs. In a co-culture model, increased expression of TNF-α and IL-6 in macrophages induced SMC calcification in a paracrine manner [43]. The atheroprotective and anti-calcific effects of osteoprotegerin (OPG) have also been associated with receptor activator of NF-κB ligand (RANKL) modulation of IL-6 production [45]. In this study, vascular smooth muscle cells from ApoE$^{-/-}$OPG$^{-/-}$ mice showed increased chondrogenic differentiation and elevated IL-6 levels in response to RANKL treatment and decreased calcification after ablation of RANKL signalling. Moreover, increased expression of IL-6 has been associated with human calcific aortic valve disease and phosphate-induced mineralization of mouse valve interstitial cells was dependent on IL-6 [46]. The NF-κB pathway was also implicated on IL-6-associated mineralization in this study. With respect to the contribution of the diseased environment to altered responses to cytokines, a recent study described an amplification autocrine loop involving IL-6 and basic calcium phosphate crystal in promoting calcification associated with experimental osteoarthritis: the increased production of IL-6 was mediated partially through STAT 3 and PI3 kinase [47].

The molecular analysis in this study was based on markers signifying three progressive phases of chondrogenesis. Thus, the significant upregulation of key genes in chondrogenesis in ApoE$^{-/-}$ VSCs in the presence of IL-6 at different stages of chondrogenic differentiation reveals that this cytokine plays a central pathological role in the atherosclerotic microenvironment. Although VSCs do not normally calcify in vivo they possess a differentiation potential which is responsive to cytokines and makes them capable of formation of ectopic bone in aortae. The differentiation of ApoE$^{-/-}$ VSCs in the presence of IL-6 to chondrocytes characterized in this study and the temporal changes observed in gene expression largely paralleled the pattern of extensive calcification in vivo occurring in atherosclerosis. Sequential gene expression patterns which closely regulate cell-cell and cell-matrix interactions leading to alterations at morphological and metabolic levels during development of cartilage [48] are not only mirrored during deposition of calcified matrix in the atherogenic processes but also to some extent during commitment of VSCs to the endochondral pathway.

Taken together, it is clear from this study that endochondral ossification and calcification in atherosclerosis is a complex interplay of a number of factors, each contributing differently to the process. It can be concluded that a major contributing factor is the intrinsic capacity of MSCs and VSCs derived from atherosclerotic mice to calcify. Nonetheless, this study also demonstrated that the environment in which cells are predifferentiated and the actual host environment drive the implanted constructs to form bone or premature bone, bone marrow, calcified cartilage, and promote infiltration of blood vessels. This study also revealed that in the presence of pro-inflammatory cytokines, IL-6 in particular, released by surrounding or localized inflammatory cells, ApoE$^{-/-}$ VSCs may become more permissive to this microenvironment and commit to the chondrogenic differentiation pathway leading to endochondral ossification.

Acknowledgments

The authors thank Dr. Xizhe Chen for his assistance and technical contribution and Dr. Shirley Hanley for assistance with flow cytometry. This work was supported by the Irish Research Council for Science, Engineering and Technology and Science Foundation Ireland under Grant No. 09/SRC/B1794.

Author Contributions

A.L.: Conception and design, Collection and/or assembly of data, Data analysis and interpretation, Manuscript writing, Final approval of manuscript; A.O.: Conception and design, Data analysis and interpretation, Final approval of manuscript; E.F.: Provision of study material, Data analysis and interpretation, Manuscript writing, Final approval of manuscript; J.P.: Data analysis and interpretation, Final approval of manuscript; F.O.: Provision of study material or patients, Final approval of manuscript; T.O'Brien, F.B.: Data analysis and interpretation, Final approval of manuscript; M.M.: Conception and design, Data analysis and interpretation, Manuscript writing, Final approval of manuscript.

Potential Conflicts of Interest

The authors indicate no potential conflicts of interests.

References

1 Gomez-Gaviro MV, Lovell-Badge R, Fernandez-Aviles F et al. The vascular stem cell niche. J Cardiovasc Transl Res 2012;5:618–630.

2 Torsney E, Xu Q. Resident vascular progenitor cells. J Mol Cell Cardiol 2011;50:304–311.

3 Klein D, Weisshardt P, Kleff V et al. Vascular wall-resident CD44 + multipotent stem cells give rise to pericytes and smooth muscle cells and contribute to new vessel maturation. PLoS One 2011;6:e20540.

4 Zengin E, Chalajour F, Gehling UM et al. Vascular wall resident progenitor cells: A source for postnatal vasculogenesis. Development 2006;133:1543–1551.

5 Tonlorenzi R, Dellavalle A, Schnapp E et al. Isolation and characterization of mesoangioblasts from mouse, dog, and human tissues. Curr Protoc Stem Cell Biol 2007; Chapter 2:Unit 2B 1.

6 Crisan M, Yap S, Casteilla L et al. A perivascular origin for mesenchymal stem cells in multiple human organs. Cell Stem Cell 2008;3:301–313.

7 da Silva Meirelles L, Chagastelles PC, Nardi NB. Mesenchymal stem cells reside in virtually all post-natal organs and tissues. J Cell Sci 2006;119:2204–2213.

8 Alexopoulos N, Raggi P. Calcification in atherosclerosis. Nat Rev Cardiol 2009;6:681–688.
9 Rajamannan NM, Bonow RO, Rahimtoola SH. Calcific aortic stenosis: An update. Nat Clin Pract Cardiovasc Med 2007; 4:254–262.
10 Johnson RC, Leopold JA, Loscalzo J. Vascular calcification: Pathobiological mechanisms and clinical implications. Circ Res 2006;99:1044–1059.
11 Fukagawa M, Kazama JJ. The making of a bone in blood vessels: from the soft shell to the hard bone. Kidney Int 2007;72:533–534.
12 Li R, Mittelstein D, Lee J et al. A dynamic model of calcific nodule destabilization in response to monocyte- and oxidized lipid-induced matrix metalloproteinases. Am J Physiol Cell Physiol 2012;302:C658–665.
13 Farrington-Rock C, Crofts NJ, Doherty MJ et al. Chondrogenic and adipogenic potential of microvascular pericytes. Circulation 2004;110:2226–2232.
14 Greenow K, Pearce NJ, Ramji DP. The key role of apolipoprotein E in atherosclerosis. J Mol Med 2005;83:329–342.
15 Farrell E, van der Jagt OP, Koevoet W et al. Chondrogenic priming of human bone marrow stromal cells: a better route to bone repair? Tissue Eng Part C Methods 2009;15:285–295.
16 Sudres M, Norol F, Trenado A et al. Bone marrow mesenchymal stem cells suppress lymphocyte proliferation in vitro but fail to prevent graft-versus-host disease in mice. J Immunol 2006;176:7761–7767.
17 Nayak RC, Berman AB, George KL et al. A monoclonal antibody (3G5)-defined ganglioside antigen is expressed on the cell surface of microvascular pericytes. J Exp Med 1988; 167:1003–1015.
18 Neuhuber B, Gallo G, Howard L et al. Reevaluation of in vitro differentiation protocols for bone marrow stromal cells: Disruption of actin cytoskeleton induces rapid morphological changes and mimics neuronal phenotype. J Neurosci Res 2004;77:192–204.
19 Parhami F, Basseri B, Hwang J et al. High-density lipoprotein regulates calcification of vascular cells. Circ Res 2002;91:570–576.
20 Lacey DC, Simmons PJ, Graves SE et al. Proinflammatory cytokines inhibit osteogenic differentiation from stem cells: Implications for bone repair during inflammation. Osteoarthr Cartil 2009;17:735–742.
21 Halfon S, Abramov N, Grinblat B et al. Markers distinguishing mesenchymal stem cells from fibroblasts are downregulated with passaging. Stem Cells Dev 2011;20:53–66.
22 Houlihan DD, Mabuchi Y, Morikawa S et al. Isolation of mouse mesenchymal stem cells on the basis of expression of Sca-1 and PDGFR-alpha. Nat Protoc 2012;7:2103–2111.
23 Canfield AE, Doherty MJ, Wood AC et al. Role of pericytes in vascular calcification: A review. Z Kardiol 2000;89(Suppl 2):20–27.
24 Crisan M, Chen CW, Corselli M et al. Perivascular multipotent progenitor cells in human organs. Ann NY Acad Sci 2009;1176:118–123.
25 Howson KM, Aplin AC, Gelati M et al. The postnatal rat aorta contains pericyte progenitor cells that form spheroidal colonies in suspension culture. Am J Physiol Cell Physiol 2005;289:C1396–1407.
26 Vasuri F, Fittipaldi S, Pasquinelli G. Arterial calcification: Finger-pointing at resident and circulating stem cells. World J Stem Cells 2014;6:540–551.
27 Iwata H, Manabe I, Nagai R. Lineage of bone marrow-derived cells in atherosclerosis. Circ Res 2013;112:1634–1647.
28 Ruan C, Shen Y, Chen R et al. Endothelial progenitor cells and atherosclerosis. Front Biosci (Landmark Ed). 2013;18:1194–1201.
29 Cabbage S, Ieronimakis N, Preusch M et al. Chlamydia pneumoniae infection of lungs and macrophages indirectly stimulates the phenotypic conversion of smooth muscle cells and mesenchymal stem cells: Potential roles in vascular calcification and fibrosis. Pathog Dis 2014;72:61–69.
30 Ergun S, Tilki D, Klein D. Vascular wall as a reservoir for different types of stem and progenitor cells. Antioxid Redox Signal 2011; 15:981–995.
31 Yang S, Eto H, Kato H et al. Comparative characterization of stromal vascular cells derived from three types of vascular wall and adipose tissue. Tissue Eng Part A 2013; 19:2724–2734.
32 Tang Z, Wang A, Yuan F et al. Differentiation of multipotent vascular stem cells contributes to vascular diseases. Nat Commun 2012;3:875.
33 Wang W, Li C, Pang L et al. Mesenchymal stem cells recruited by active TGFbeta contribute to osteogenic vascular calcification. Stem Cells Dev 2014;23:1392–1404.
34 Yan J, Stringer SE, Hamilton A et al. Decorin GAG synthesis and TGF-beta signaling mediate Ox-LDL-induced mineralization of human vascular smooth muscle cells. Arterioscler Thromb Vasc Biol 2011;31:608–615.
35 Demer LL, Tintut Y. Vascular calcification: Pathobiology of a multifaceted disease. Circulation 2008;117:2938–2948.
36 Abedin M, Tintut Y, Demer LL. Mesenchymal stem cells and the artery wall. Circ Res 2004;95:671–676.
37 Farrell E, Both SK, Odorfer KI et al. In-vivo generation of bone via endochondral ossification by in-vitro chondrogenic priming of adult human and rat mesenchymal stem cells. BMC Musculoskelet Disord 2011;12:31.
38 Yang W, Yang F, Wang Y et al. In vivo bone generation via the endochondral pathway on three-dimensional electrospun fibers. Acta Biomater 2013;9:4505–4512.
39 Hansson GK. Inflammation, atherosclerosis, and coronary artery disease. N Engl J Med 2005;352:1685–1695.
40 Sage AP, Tintut Y, Demer LL. Regulatory mechanisms in vascular calcification. Nat Rev Cardiol 2010;7:528–536.
41 Heldens GT, Blaney Davidson EN, Vitters EL et al. Catabolic factors and osteoarthritis-conditioned medium inhibit chondrogenesis of human mesenchymal stem cells. Tissue Eng Part A 2012;18:45–54.
42 Murakami S, Lefebvre V, de Crombrugghe B. Potent inhibition of the master chondrogenic factor Sox9 gene by interleukin-1 and tumor necrosis factor-alpha. J Biol Chem 2000;275:3687–3692.
43 Deuell KA, Callegari A, Giachelli CM et al. RANKL enhances macrophage paracrine pro-calcific activity in high phosphate-treated smooth muscle cells: Dependence on IL-6 and TNF-alpha. J Vasc Res 2012;49:510–521.
44 Pricola KL, Kuhn NZ, Haleem-Smith H et al. Interleukin-6 maintains bone marrow-derived mesenchymal stem cell stemness by an ERK1/2-dependent mechanism. J Cell Biochem 2009;108:577–588.
45 Callegari A, Coons ML, Ricks JL et al. Increased calcification in osteoprotegerin-deficient smooth muscle cells: Dependence on receptor activator of NF-κB ligand and interleukin 6. J Vasc Res 2014;51:118–131.
46 El Husseini D, Boulanger MC, Mahmut A et al. P2Y2 receptor represses IL-6 expression by valve interstitial cells through Akt: implication for calcific aortic valve disease. J Mol Cell Cardiol 2014;72:146–156.
47 Nasi S, So A, Combes C et al. Interleukin-6 and chondrocyte mineralisation act in tandem to promote experimental osteoarthritis. Ann Rheum Dis. 2015 Aug 7. pii: annrheumdis-2015-207487. doi: 10.1136/annrheumdis-2015-207487. [Epub ahead of print]
48 Kronenberg HM. Developmental regulation of the growth plate. Nature 2003;423: 332–336.

See www.StemCells.com for supporting information available online.